

Assimilation of HY-2A Scatterometer Ambiguous Winds Based on Feature Thinning

Boheng DUAN*, Weimin ZHANG, Xiaoqun CAO, Yi YU, and Haijin DAI

Academy of Ocean Science and Engineering, National University of Defense Technology, Changsha 410073

(Received October 25, 2016; in final form February 17, 2017)

ABSTRACT

This paper focuses on the data assimilation methods for sea surface winds, based on the level-2B HY-2A satellite microwave scatterometer wind products. We propose a new feature thinning method, which is herein used to screen scatterometer winds while maintaining the key structure of the wind field in the process of data thinning for high-resolution satellite observations. We also accomplish feeding the ambiguous wind solutions directly into the data assimilation system, thus making better use of the retrieved information while simplifying the assimilation process of the scatterometer products. A numerical simulation experiment involving Typhoon Danas shows that our method gives better results than the traditional approach. This method may be a valuable alternative for operational satellite data assimilation.

Key words: data assimilation, HY-2A scatterometer, feature thinning, ambiguous winds

Citation: Duan, B. H., W. M. Zhang, X. Q. Cao, et al., 2017: Assimilation of HY-2A scatterometer ambiguous winds based on feature thinning. *J. Meteor. Res.*, **31**(4), 720–730, doi: 10.1007/s13351-017-6165-8.

1. Introduction

The scatterometer is a non-imaging satellite radar sensor, which collects sea surface roughness information by measuring the sea surface backscattering coefficient, and then the sea surface wind vector can be retrieved. Sea surface wind data are important as they supply as boundary conditions for atmospheric and marine environment numerical prediction models. Unfortunately, there is a serious lack of information on surface winds, especially for tropical cyclones (Rogers et al., 2003), and wind measurements from buoys and ships are limited, discretized, and unevenly distributed. Fortunately, the satellite scatterometer can effectively compensate for the shortcomings of these traditional methods of measurement, making it possible for all-day, all-weather global exploration, and has become an effective means of obtaining sea surface wind data. The HY-2A satellite is a first-generation marine dynamics remote-sensing satellite launched in China. It can provide high-resolution and high-precision sea surface wind data over oceanic areas. The global daily average sea area coverage of HY-2A satellite observations is about 95%. The retrieved sea sur-

face wind field on 4 October 2013 is shown in Fig. 1.

Since the launch of the first operational scatterometer satellite, Seasat, in the United States in 1978, a number of satellite scatterometers have been employed for operation. The scatterometer satellites currently in operation include the European Space Agency's METOP series, India Oceansat-2, ScatSat, and China's HY-2 series. Scatterometer data were first used in a numerical weather forecasting operational system in 1998, when the ECMWF

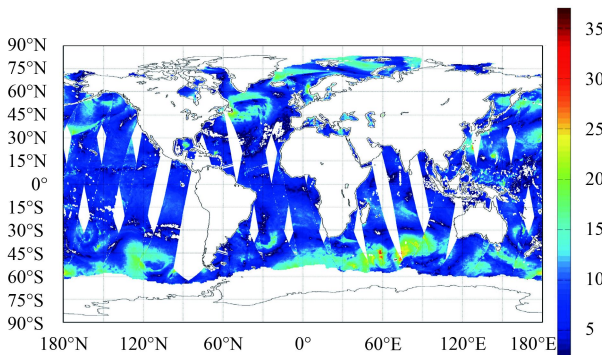


Fig. 1. Sea surface wind field (m s^{-1}) on 4 October 2013 retrieved from the HY-2A satellite scatterometer.

Supported by the State Key Development Program for Basic Research of China (4175094).

*Corresponding author: bhduan@foxmail.com.

©The Chinese Meteorological Society and Springer-Verlag Berlin Heidelberg 2017

incorporated ERS-1 scatterometer data into its global three-dimensional variational system (Andersson et al., 1998). Previous work has shown that scatterometer data have significant impacts on the analysis and forecasting of tropical cyclones (Prasad et al., 2013). Since the *HY-2A* scatterometer was put into operation in 2011, it has accumulated a large amount of valuable surface wind observations (Lin et al., 2013). However, to date, work on *HY-2A* scatterometer data has mainly focused on data preprocessing (Zhang et al., 2013) and wind retrieval (Lin et al., 2013). Yu et al. (2015) analyzed the effect of the use of synoptic *HY-2A* scatterometer data on the forecasting of Typhoon Blavan, but in general, the assimilation of *HY-2A* scatterometer data is not at an advanced stage, and the operational use of these data is not yet mature. In the level-2B data products of the *HY-2A* scatterometer released by the National Satellite Marine Application Center of China, each of the non-empty wind vector cells (WVCs) contains a group of ambiguous wind vectors retrieved from information such as back scattering coefficient measurements, azimuth, incidence, and polarization pattern. Also given is one fixed wind vector, which is determined by the ambiguity removal algorithm. How to make good use of the *HY-2A* scatterometer data products in an operational setting is a very important issue.

Current satellite observations generally have high temporal and spatial resolutions. For example, the horizontal resolution of the *HY-2A* scatterometer has reached 25 km. If such high-resolution observations are brought directly into the assimilation system, the computational overhead will be greatly increased. In addition, high-resolution data will inevitably produce some spatial correlation errors in the observations (Ochotta et al., 2005). Therefore, the use of an observational thinning technique has become a key technological development in the pretreatment stage of satellite data assimilation. It plays an important role in improving the effect of data assimilation, and different thinning algorithms should be designed for different types of satellite observations. At present, the most common way to thin satellite observations is by using a temporal or spatial sampling method, which distributes observations evenly in time and space. Alternatively, a “super-observation” method can be used, where a region of observations is weighted averagely. Ochotta et al. (2005) proposed two thinning methods: one in which the observational data are clustered according to the observed spatial position and observed data, and then the center of each cluster is retained; and the other iteratively estimates the redundancy of the observation set and the most redundant observations in the data-set are removed. Li et al. (2010) proposed a thinning

scheme that accounts for the background error covariance information of the model, which minimizes the analysis error variance by selecting observations. Bauer et al. (2011) proposed a method based on singular vectors that identifies sensitive regions for satellite observations. The non-sensitive regions use a conventional thinning method, while the sensitive regions retain more observations. Gratton et al. (2015) proposed a thinning method based on hierarchical observations, starting with the lowest (sparse) layer and adding observations gradually based on a posteriori error estimates. However, these methods have no special consideration for the vector type observation. In this paper, based on the wind data of the level-2B products of the *HY-2A* scatterometer, a feature thinning method based on the wind vector field is proposed. To achieve the aim of thinning and decorrelation, the main idea of this algorithm is to retain the strong structural characteristics of the wind field observations, while the non-structural areas use the weighted average of observations. Through a numerical simulation experiment of a typhoon case, we show how the precision of the prediction of the typhoon’s path is greatly improved, as compared to when using the traditional thinning method.

The wind vector solution obtained by inversion of the scatterometer data is not unique. To obtain a wind vector closest to the real solution as the fixed wind vector solution of the inversion, we need to eliminate these ambiguous solutions. The *HY-2A* scatterometer uses the circle median filtering method to determine the unique wind vector solution (Lin et al., 2010). However, the circle median filtering algorithm requires more than half of the initial wind field to be correct, and different choices for the weight of the ambiguous winds will have a certain effect on the process of the ambiguity removal. Vogelzang (2007) incorporated numerical forecasting background wind field information, and proposed the use of a two-dimensional variational assimilation method to carry out wind field ambiguity removal, achieving good results. However, by using the two-dimensional variational method to eliminate the ambiguity, the error information of the external background wind field is brought into the fixed wind of the scatterometer, which is directly substituted into the assimilation system, thus inevitably affecting the assimilation result. Based on the weather research and forecasting model and its three-dimensional variational data assimilation platform (WRFDA), this paper reports the direct assimilation of the level-2B ambiguous wind vectors of the *HY-2A* scatterometer, avoiding the introduction of the external background field error before assimilation. The numerical simulation results of the

typhoon case show that the direct assimilation method is more effective than the assimilation of fixed wind. This can provide a theoretical reference for the use of *HY-2A* scatterometer data into a data assimilation system.

Following this introduction, a brief description of the *HY-2A* scatterometer and wind products is given in Section 2. Section 3 introduces the specific flow of the thinning algorithm. In Section 4, we present the definite operators of the direct solution of the fuzzy solution of the scatterometer. In Section 5, we use a numerical simulation experiment of a typhoon case to study the feature thinning (FT) method and the direct assimilation of ambiguous wind vectors, and the results are compared with those of conventional assimilation methods. Finally, a conclusion is provided in Section 6.

2. *HY-2A* scatterometer and L2B wind product

The *HY-2A* satellite revolves around earth at a height of 963 km and has a sun-synchronous orbit with an inclination of 99.3°. The descending intersection point of the satellite is 0600 UTC. The *HY-2A* scatterometer employs a Ku-band (13.256 GHz) circular cone scan model. The swath is 1800 km (Wang et al., 2012) and it uses two polarization beams—the horizontal polarization beam at an incident angle of 41°, and the vertical polarization beam at an incident angle of 49°.

The level-2B products of the *HY-2A* scatterometer are organized by its orbit, which are split into different files every time when it passes the descending intersection point. The WVC of the level-2B product can be indexed by its row and column number, where the direction of the row is perpendicular to the orbit and the column is along the orbit. Sea surface roughness information is captured by measuring the scatterometer backscatter, and thus the wind vector can be retrieved by using the geophysical model functions (GMFs). The GMFs are largely based on empirical fits to the data (Hilburn et al., 2006).

However, owing to the dual nature between the backward scattering cross-section and the azimuth, radar echo signal anisotropy, nonlinearity of the geophysical model function, and signal noise of observation, the wind direction of a wind vector solution is not unique; in this set of multiple wind direction solutions, only one direction is closer to the true wind direction and all other directions are ambiguous, which we refer to as “ambiguities.” Traditionally, before we use this wind product in our data assimilation system, the ambiguity of the wind vector solution should be removed so that only one wind direction remains. Multiple wind directional ambiguity removal

methods have been developed to de-alias the direction, such as the circle median filter, which is used in the wind retrieval of the *HY-2A* scatterometer to provide one fixed surface wind vector. The level-2B products provide both the fixed wind vector and four ambiguous wind vectors for each WVC with a resolution of 25 km.

3. Feature thinning of *HY-2A* scatterometer wind

The use of observational data is of great significance for improving the initial conditions of numerical prediction. With the development of observation methods, the temporal and spatial resolution of observed data is getting higher and higher. However, due to the theoretical framework of assimilation and the limitation of numerical prediction systems, the observational data must be dealt with cautiously. On the one hand, not only does the assimilation of more observations mean more cost in terms of computing time, but it also greatly increases the storage cost as well as the transmission overhead of the data; on the other hand, the higher temporal and spatial resolutions will greatly increase the correlation between the observations, while in most data assimilation systems, observations are assumed to be uncorrelated. Therefore, it is necessary to dilute the observational data, remove the redundant part, and preserve the most important information among them (Ochotta et al., 2005).

When compressing large datasets, retaining the main features of the data is a key issue in many disciplines. At present, in assimilation systems, the most commonly used thinning method is “window sampling” or “super-observation,” as shown in Fig. 2. In a 2×2 grid, window sampling only selects one of the observations in one grid, while super-observation measures the observational data in the window to obtain a new observation by weighted averaging.

Conventional thinning methods can reduce the correlation between observations to some extent, but global smoothing can destroy some of the structural characteristics of the data field. In many cases, these structural features often contain some key information, such as the wind field vortex structure of typhoons. Based on the weakness of this method, this paper proposes an FT method for the vector wind field. Its basic idea is that, in the observation, when a point is similar to the surrounding points, the redundancy of this point is considered to be high, and the algorithm merges the observation of this point with the surrounding points. On the other hand, when the difference from the surrounding points is large, it is a feature observation that the algorithm keeps at that

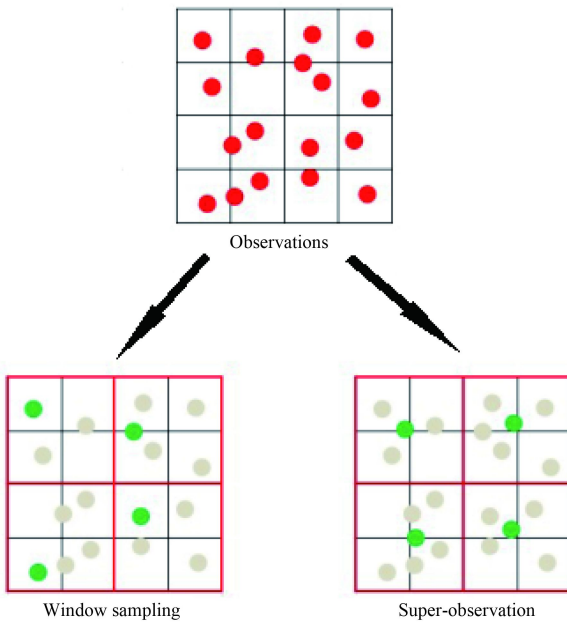


Fig. 2. Conventional thinning schemes for observations.

point. The flow of the FT algorithm is shown in Fig. 3.

The FT algorithm consists of the following steps:

(1) Meshing: In order to facilitate the calculation of the computer, the first step is to mesh the data in accordance with the geographical location of the regular grid, so that each grid has no more than one observation. The HY-2A scatterometer level-2B product data file is organized in units of tracks, and each data element can be marked by the row and column numbers of the WVC. The row number (m) and the column number (n) of the WVC are 1624 and 76, respectively. Therefore, each WVC is a grid cell.

(2) Cluster initialization: The entire grid needs to be initialized before the algorithm begins, so that each grid cell W_i belongs to a separate cluster C_i , expressed as

$$W_i \Rightarrow C_i,$$

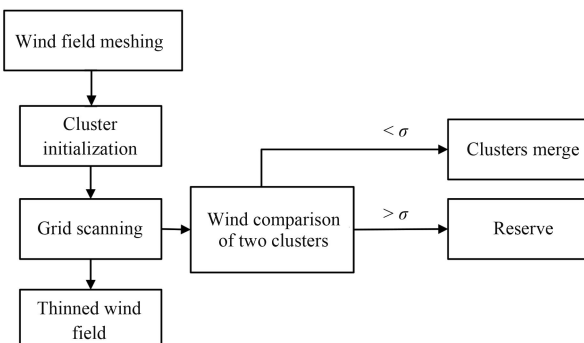


Fig. 3. Flow of the feature thinning algorithm. Note that σ is the proportional threshold.

where i is the index of the cluster, and

$$i = (x - 1) \times n + y, \quad 1 \leq x \leq m, \quad 1 \leq y \leq n,$$

in which (x, y) is the row and column index of the grid cell. Each cluster contains the wind vector (u_i, v_i) and latitude and longitude coordinate $(\text{lat}_i, \text{lon}_i)$ information within the grid cell:

$$C_i = \{u_i, v_i; \text{lat}_i, \text{lon}_i\}.$$

(3) Grid scanning: This involves scanning the whole grid following the order from the left to the right, and from the top to the bottom. The specific process of scanning involves comparing the cluster C_j to which the right (lower) grid belongs with the cluster C_i to which the current grid belongs. If

$$\frac{(u_i - u_j, v_i - v_j)}{(u_i, v_i)} \leq \sigma,$$

that is, if the wind vector difference of two clusters does not exceed a certain proportion threshold σ , then the two clusters C_i and C_j are combined. The wind component and the latitude and longitude coordinates of the new cluster $C(i, j)$ are the average of two clusters; namely,

$$C_{(i,j)} = \{\bar{u}_{(i,j)}, \bar{v}_{(i,j)}, \bar{\text{lat}}_{(i,j)}, \bar{\text{lon}}_{(i,j)}, \},$$

where (i, j) denotes the index of all the grids contained in the new cluster. This then updates the clusters belonging to the two grids; that is,

$$\begin{aligned} W_i &\Rightarrow C_{(i,j)}; \\ W_j &\Rightarrow C_{(i,j)}. \end{aligned}$$

If the wind vector difference of two clusters exceeds the proportional threshold σ , that is,

$$\frac{(u_i - u_j, v_i - v_j)}{(u_i, v_i)} > \sigma,$$

the cluster to which the two grids belong is reserved, and the search process is moved to the next grid cell. This scanning step can be performed iteratively. That is, after the entire grid has completed a scan cycle, the entire mesh cluster is updated and the grid scan is re-executed on the basis of the new cluster. The iteration stop condition can be either set to the maximum number of iterations or to abort when the grid cluster is no longer updated.

Figure 4 is a sketch map of the wind field thinning within 5×5 grid. The algorithm starts from the first grid of the wind field and compares the wind vector of the cluster on the right side with the wind vector of the current grid cluster; if the difference exceeds the threshold, keep the second cluster. The grid below is then compared to the current grid, and if the difference is less than

the threshold, then the two clusters are merged to form a new cluster.

After completing the whole grid scan, the wind vector field composed of the new cluster is preserved, which is the wind field after the feature thinning, as shown in the lower right box of Fig. 4.

4. Direct assimilation of HY-2A scatterometer ambiguous winds

There are two ways to bring scatterometer data into a variational assimilation system (Fig. 5):

(1) The conventional method to assimilate the *HY-2A* scatterometer product uses the fixed wind that remains after the ambiguity removal step. In the process of ambiguity removal, and taking two-dimensional variational ambiguity removal (Zhang et al., 2010) as an example, background field information is incorporated. Because the background field has its own uncertainty, the ambiguity removal results are related to the background field with spatial correlation. If the fixed wind is directly assimilated into the NWP, the NWP background wind field correlation information introduced from the two-dimensional variational ambiguity removal process will be brought into the assimilation process, which will intro-

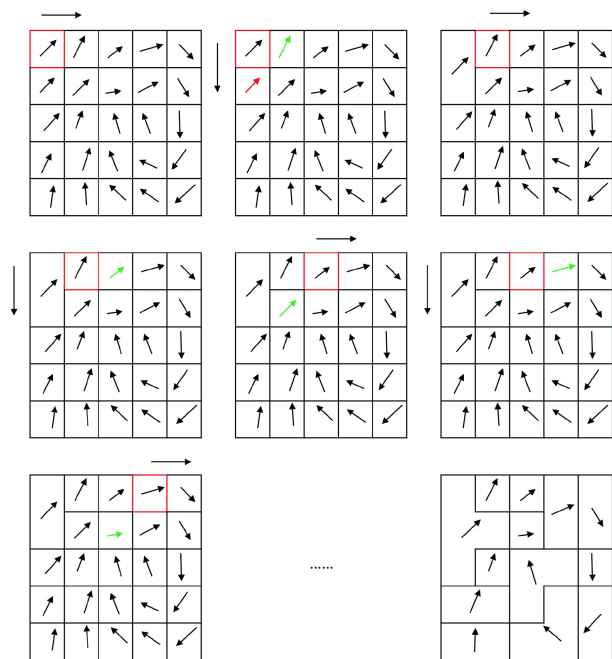


Fig. 4. Schematic diagrams of feature thinning in a 5×5 grid. The red squared frame represents the current grid being processed. The long arrow outside the box points to the grid adjacent to the current one to which it is being compared. A green arrow means that the wind vector is retained, while the red arrow means that it is going to be merged with the wind vector in the current grid.

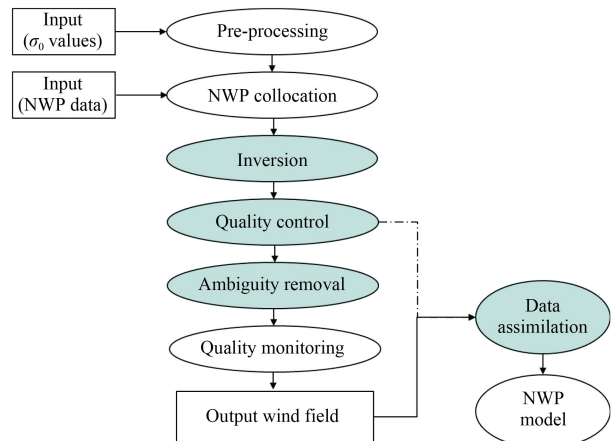


Fig. 5. The main flow of scatterometer data processing.

duce the spatial correlation error.

(2) After the inversion of the scatterometer data, the ambiguous solutions are directly introduced into the variational assimilation system without ambiguity removal, so as to avoid bringing in the background error information twice, but the objective function of the variational system needs to be redesigned.

For the level-2B wind products of the *HY-2A* scatterometer, the quality of every WVC is controlled by a 16-bit unsigned integer called `wvc_quality_flag`. The quality of the retrieved wind is determined by the number and quality of the measurement of scatterometer backscatter. If one WVC has an insufficient number of good measurements, then it is not suitable for the wind inversion. In this condition, the ninth bit of the flag is set to 1, meaning that the WVC should not be used. Compare to the C-band (5 GHz) scatterometer, the higher frequency of the Ku-band instrument allows greater sensitivity at low wind speed, but exhibits greater influence from atmospheric precipitation (Yu et al., 2015). The flag uses two bits (5 and 6) to indicate the rain condition in the WVC. If it is in a condition of strong rainfall, the WVC should not be used, either.

The inversion product of the scatterometer data is the wind vector (wind speed and wind direction), which is at a height of 10 m. Before assimilation, the wind vector needs to be converted to meridional (v) and zonal (u) wind components. The general form of the cost function of the scatterometer wind in data assimilation is shown by the formula below:

$$J = J_o^{\text{scat}} + J_b,$$

where J_b represents the deviation of the background from the analysis, and J_o^{scat} represents the deviation of the observation (scatterometer wind) from the analysis. The form of J_b is

$$J_b = \frac{1}{2} (x - x_b)^T \mathbf{B}^{-1} (x - x_b),$$

where $x = (u, v)^T$ is the analytical solution, $x_b = (u_b, v_b)^T$ is the background wind, and \mathbf{B} is the background error covariance matrix.

In order to improve the computational efficiency, the incremental δx is employed:

$$\delta x = (x - x_b) = \begin{pmatrix} \delta u \\ \delta v \end{pmatrix}.$$

The objective equation and gradient equation of observation between the fixed wind assimilation and ambiguous wind direct assimilation are shown in Table 1. The \mathbf{H} is a tangential observation operator, and it is assumed that the observation errors of the δu and δv components are estimated from the error of the wind velocity, and that the two observation error components ε are equal and unrelated. Here, given $\varepsilon = 0.5 \text{ m s}^{-1}$, for the ambiguous wind direct assimilation operator, the parameter p is an empirical parameter that gives optimal separation between multiple solutions for $p = 4$, N is the number of ambiguous winds ($N = 4$ for the HY-2A scatterometer), and i is the ambiguous wind number.

The ambiguous wind direct assimilation operator simplifies the ambiguity removal and wind components assimilation into only one step. The gradient of the assimilation operator is required during the minimization of the cost function during the variational analysis. The above modification to the observation variational cost function and its gradient is not difficult to implement in the assimilation system.

5. Typhoon numerical simulation

5.1 Data selection and parameter setting

In this paper, we select Typhoon Danas (2013) as a numerical example, which was generated in Northwest Pacific at 1400 UTC 4 October 2013, in the vicinity of 16.9°N, 145.6°E. The center's maximum wind speed was about 18 m s⁻¹, and its pressure was about 998 hPa. Danas weakened to an extratropical cyclone on 9 October. The WRFDA developed by NCAR (Barker et al., 2004) is adopted in this paper. The WRFDA system is a widely used operational system that can produce a multivariate incremental analysis in the WRF model space (Zhang et al., 2009). The center of the forecast area is 20.75°N, 141°E; the grid size of the assimilation region is 511 × 511; the horizontal resolution is 9 km; and the vertical discretization is 57 layers. The time of assimilation is based on the time window of the HY-2A scatterometer scan of the typhoon region, which was 1800 UTC 4 October 2013. Using FNL (final) global analysis data provided by the NCEP as the initial field and boundary conditions, we take the 18-h forecast adjustment from 0000 to 1800 UTC 4 October 2013 as the background field of the assimilation system. After the assimilation, a 60-h forecast is made, which is a forecast to 1800 UTC 7 October 2013. The assimilation uses the HY-2A satellite microwave scatterometer level-2B data products provided by the National Satellite Marine Application Center of China as observations, which include both the fixed winds and the ambiguous winds.

In this paper, a set of assimilation and comparison ex-

Table 1. Comparison of the fixed wind and ambiguous wind direct assimilation operator

	Fixed wind assimilation	Ambiguous wind direct assimilation
Objective equation	$J_o^{\text{scat}} = \frac{1}{2} \frac{(\mathbf{H} \delta u - \delta u^{\text{scat}})^2 + (\mathbf{H} \delta v - \delta v^{\text{scat}})^2}{\varepsilon^2}$.	$J_s^{\text{scat}} = J_s^{-\frac{1}{p}},$ $J_s = \frac{1}{2} \sum_{i=1}^N \left(\frac{(\mathbf{H} \delta u - \delta u_i^{\text{scat}})^2 + (\mathbf{H} \delta v - \delta v_i^{\text{scat}})^2}{\varepsilon^2} \right)^{-p}.$
Gradient equation	$\frac{\partial J_o^{\text{scat}}}{\partial \delta u} = \mathbf{H}^T \frac{(\mathbf{H} \delta u - \delta u^{\text{scat}})}{\varepsilon^2},$ $\frac{\partial J_o^{\text{scat}}}{\partial \delta v} = \mathbf{H}^T \frac{(\mathbf{H} \delta v - \delta v^{\text{scat}})}{\varepsilon^2}.$	$\frac{\partial J_s^{\text{scat}}}{\partial \delta u} = \frac{\partial J_o^{\text{scat}}}{\partial J_s} \frac{\partial J_s}{\partial \delta u} = \frac{-1}{p} J_s^{-1-1/p} \frac{\partial J_s}{\partial \delta u},$ $\frac{\partial J_s^{\text{scat}}}{\partial \delta v} = \frac{\partial J_o^{\text{scat}}}{\partial J_s} \frac{\partial J_s}{\partial \delta v} = \frac{-1}{p} J_s^{-1-1/p} \frac{\partial J_s}{\partial \delta v},$ $\frac{\partial J_s}{\partial \delta u} = -p \sum_{i=1}^N \left(\frac{(\mathbf{H} \delta u - \delta u_i^{\text{scat}})^2 + (\mathbf{H} \delta v - \delta v_i^{\text{scat}})^2}{\varepsilon^2} \right)^{-p-1} \cdot \frac{(\mathbf{H} \delta u - \delta u_i^{\text{scat}})}{\varepsilon^2},$ $\frac{\partial J_s}{\partial \delta v} = -p \sum_{i=1}^N \left(\frac{(\mathbf{H} \delta u - \delta u_i^{\text{scat}})^2 + (\mathbf{H} \delta v - \delta v_i^{\text{scat}})^2}{\varepsilon^2} \right)^{-p-1} \cdot \frac{(\mathbf{H} \delta v - \delta v_i^{\text{scat}})}{\varepsilon^2}.$

periments are carried out. The assimilation experiment design is shown in Table 2, in terms of the thinning scheme (traditional window sampling and feature thinning) and observation types (fixed winds and ambiguous winds).

5.2 Results and analysis

At the time of assimilation, the fixed wind field of the scatterometer in the central region of the typhoon is shown in Fig. 6a. It can be clearly seen that, in the typhoon eye area (center of the left part of Fig. 6a), the wind speed is large and the wind direction changes more violently. The typhoon vortex can be regarded as the structural feature of the wind field, which will be retained in the FT algorithm. In the non-typhoon region, the wind speed is small and the wind direction is almost unchanged. The unstructured region in the wind field will be thinned in the FT algorithm to a greater extent.

For the conventional thinning method, we use a 4×4 grid for window sampling. As shown in Fig. 6b, after the thinning process, the wind field is evenly distributed, but

the vortex structure of the typhoon eye region has clearly been destroyed. The super-observation method shows the same characteristic as the window sampling method, as can be seen in Fig. 6c. In the FT algorithm, the result of thinning depends on the variability of the wind field itself. Here, the threshold r is 0.08, and the number of iterations is 3. As shown in Fig. 6d, the structural characteristics of the vortices in the wind field after thinning are well preserved, and the distribution of the wind field is also a better reflection of the characteristics of the wind flow field.

For the direct assimilation of scatterometer ambiguous winds, the initial wind field is uncertain before the assimilation, and the structure of the wind field is uncertain. Therefore, an initial wind field needs to be determined for the thinning of the ambiguous winds. Here, we take the NWP background wind at the same time as the initial wind field to carry out the FT, and then retain the ambiguous winds corresponding to the position of the background wind after the FT process. The retained am-

Table 2. Data assimilation experiment design

Experiment name	Assimilation system	Thinning scheme	Observation type
Traditional thinning		Window sampling	Fixed winds
Feature thinning		Feature thinning	Fixed winds
Ambiguity traditional thinning	WRF-3DVAR	Window sampling	Ambiguous winds
Ambiguity feature thinning		Feature thinning	Ambiguous winds

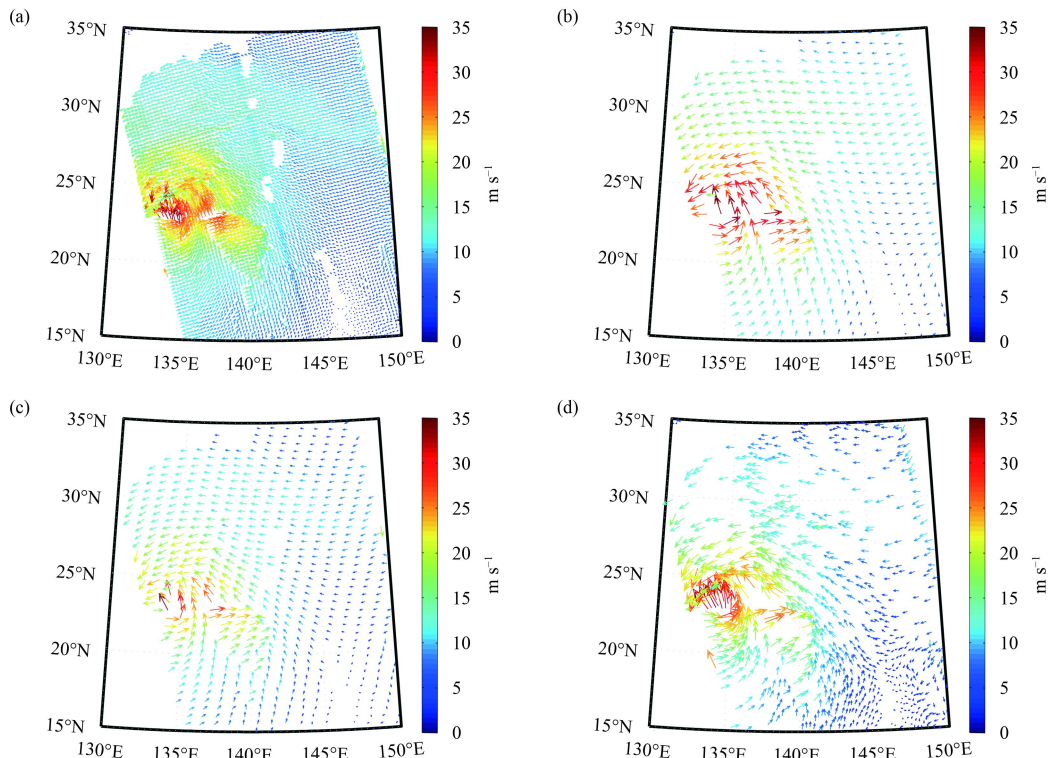


Fig. 6. Wind field of Typhoon Danas: (a) full data, (b) window sampling, (c) super-observation, and (d) feature thinning.

biguous winds are then assimilated into the assimilation system as observation.

We use the FNL global analysis wind field as a reference, and a comparison of the bias (mean), root-mean-square value, and standard deviation (STD) of the u and v components is made for the HY-2A scatterometer fixed winds from the regular thinning, FT, as shown in Fig. 7. The wind field after FT has a wider range of wind speed and smaller bias. However, the FT scheme shows a slightly larger RMS and STD for the u component. This is mainly caused by the wind field after FT retaining more gradient samples of large gradient and variance, while it is much smoother in the reanalysis wind field.

Figure 8 shows the O/B (observation versus background) and O/A (observation versus analysis) comparison of the bias, RMS, and STD of the u and v components of the HY-2A scatterometer fixed winds after assimilation. Since the window sampling scheme filters out most of the sharp features (with high gradient and variance) of the wind field, it is smoother and more compatible with the background wind field compared to the feature thinning scheme. However, smaller innovation (O–B) and analysis residual (O–A) of the wind components does not mean a better analysis. Other aspects, such as pressure error and improvement to the forecast, should also be considered.

Figure 9 shows the pressure error at the 10-m height of the eye of Typhoon Danas at the analysis time. The fixed wind assimilation based on FT (Fig. 9b) does not show a big difference with the traditional thinning scheme (Fig. 9a). However, the direct assimilation of ambiguous

winds (Figs. 9c, d) improves the analysis of pressure significantly compared to the assimilation of fixed wind.

Figure 10 shows the true and forecasted typhoon paths in different experiments. It is apparent that the location of the typhoon center based on different thinning schemes is very close to the control experiment (with no assimilation of the scatterometer wind) at the time of the assimilation, but the path of wind assimilation is closer to the true path than that of the control experiment. In order to better compare the accuracy of the assimilation experi-

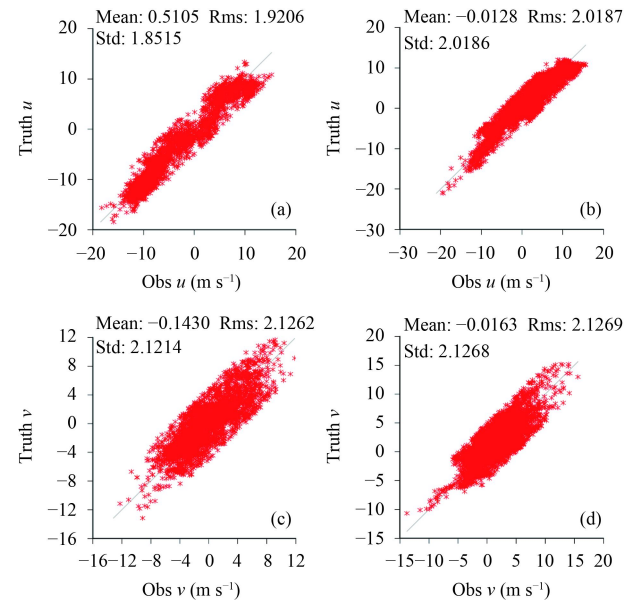


Fig. 7. Comparison of the bias, root-mean-square value, and standard deviation of the u (zonal; a, b) and v (meridional; c, d) wind components: (a, c) window sampling and (b, d) feature thinning.

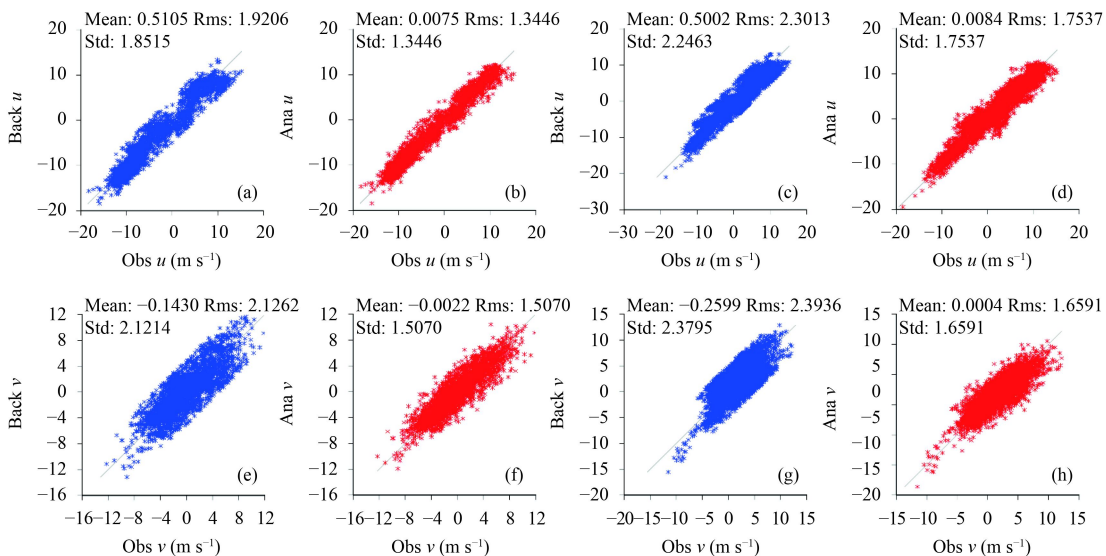


Fig. 8. O/B and O/A comparison of the bias, root-mean-square value, and standard derivation of the u (zonal; a–d) and v (meridional; e–h) wind components: (a, b, e, f) window sampling and (c, d, g, h) feature thinning.

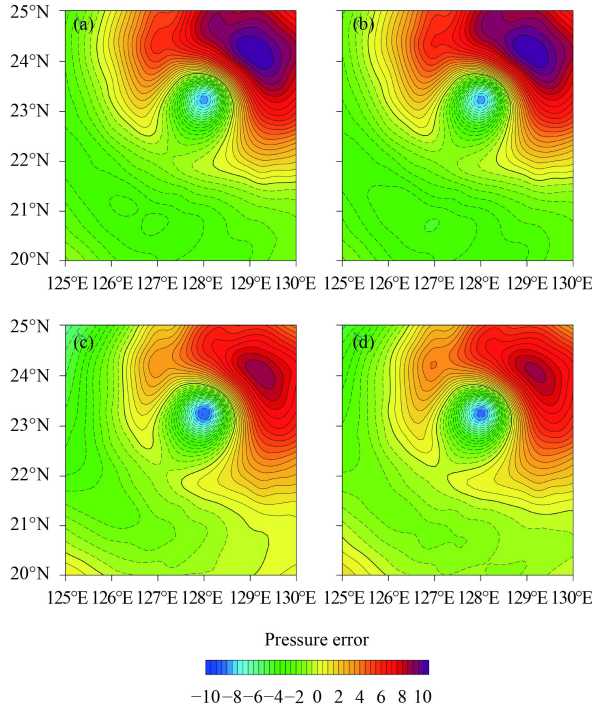


Fig. 9. Pressure error of the eye of Typhoon Danas at the analysis time: (a) fixed wind assimilation based on traditional window sampling, (b) fixed wind assimilation based on feature thinning, (c) direct assimilation of ambiguous winds based on traditional window sampling, and (d) direct assimilation of ambiguous winds based on feature thinning.

ment with the typhoon moving path, Fig. 10 also gives the error of the forecasted typhoon path. It is shown that, with an increase in forecast time, the typhoon path error of the assimilation experiments becomes obviously smaller than that of the control experiment. Generally, the forecasted paths of the direct assimilation of ambiguous winds are better than that of the fixed wind using the same thinning scheme, and the FT schemes are better than the traditional thinning schemes using the same type of wind.

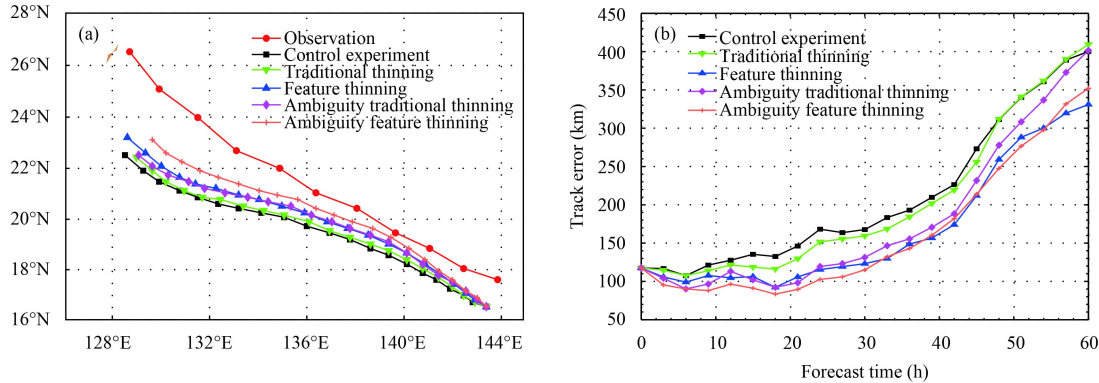


Fig. 10. Forecasted (a) path and (b) track errors of Typhoon Danas.

The intensity of the typhoon based on the different schemes is compared in Fig. 11. As can be seen, the direct assimilation of ambiguous winds improves the pressure forecast of the typhoon eye, as compared to that of fixed wind. However, the result of the maximum wind speed forecast is quite mixed. The benefit of the FT does not show up in the simulation of the typhoon's intensity. One possible reason for this may be that the FT scheme mainly improves the vortex structure of the typhoon eye, which has a considerable impact on the track forecast. Meanwhile, the effect of the vortex structure on the typhoon intensity forecast remains unknown.

The scatterometer winds have a small number of observable deviations, especially at the edge of the swath, as shown in Fig. 6. These deviation observations are difficult to eliminate by using the thinning process, and in the FT algorithm these observations with bias will be retained as a feature vector, which will modulate the effect of assimilation. The objective function of the direct assimilation of ambiguous winds will pick out the solution closest to the model background field, so it is more harmonious with the model background than the fixed wind. The prediction of the typhoon's path shows the advantage of direct assimilation with ambiguous winds (Fig. 10).

6. Summary

Based on the NCAR's WRFDA system, three-dimensional variational data assimilation of the fixed wind and ambiguous wind of the wind products of the HY-2A scatterometer is realized. The experimental results show that the FT method proposed in this paper is able to preserve the characteristics of the wind field better than the traditional thinning method, whilst at the same time removing the redundancy of the observation. The direct assimilation of the ambiguous winds avoids the error informa-

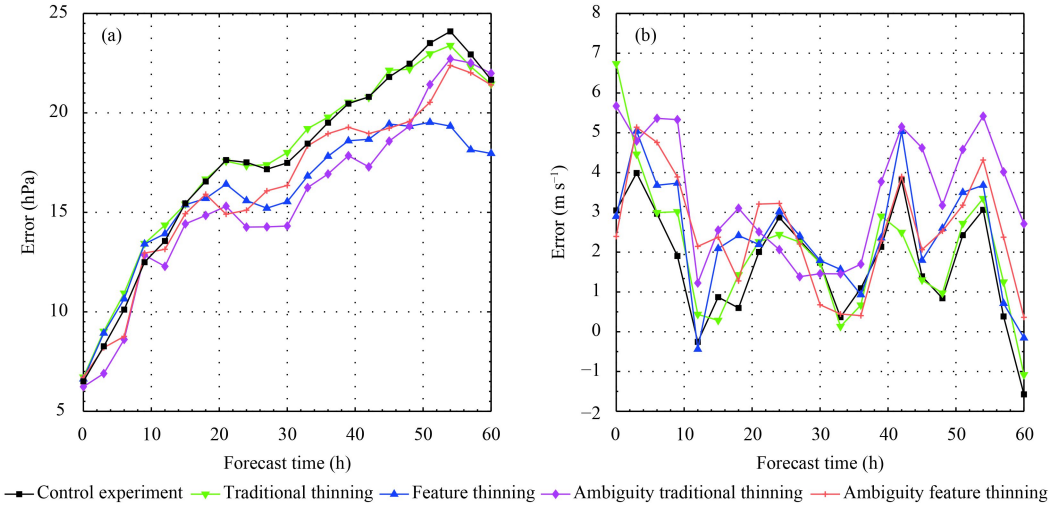


Fig. 11. Forecast errors of (a) pressure and (b) maximum wind speed of the typhoon eye.

tion of the background field being introduced into the ambiguity removal process, and makes the analysis more coordinated with the model background field. This is well verified by a numerical simulation experiment of a typhoon case.

In the next step in this avenue of research, we need to make further improvements to the FT algorithm, because a small number of obvious errors in the observation field will be considered as the feature vector, thus modulating the effect of assimilation. Therefore, it is necessary to denoise the observation field before the FT algorithm is executed. In addition, the relationship between the degree of thinning of the observation field and the threshold value needs to be proved by a large number of experiments. Moreover, the computational cost of the FT algorithm increases exponentially with an increase in the threshold value, so there is still possibility for improvement in the algorithm's optimization, especially parallel optimization. For the assimilation of scatterometer ambiguous winds, the weighting information of each ambiguous solution in the inversion process is not considered in the assimilation. Therefore, next, the ambiguous solution weighting information should be introduced into the assimilation operator. To introduce the multiple solution scheme (Zhang et al. 2010) into the assimilation of the scatterometer data is also a problem to be studied in the future.

Acknowledgments. The authors would like to thank the National Satellite Marine Application Center of China for providing the HY-2A satellite microwave scatterometer level-2B data products.

REFERENCES

- Andersson, E., J. Haseler, P. Undén, et al., 1998: The ECMWF implementation of three-dimensional variational assimilation (3D-Var). III: Experimental results. *Quart. J. Roy. Meteor. Soc.*, **124**, 1831–1860, doi: [10.1002/\(ISSN\)1477-870X](https://doi.org/10.1002/(ISSN)1477-870X).
- Barker, D. M., W. Huang, Y.-R. Guo, et al., 2004: A three-dimensional variational data assimilation system for MM5: Implementation and initial results. *Mon. Wea. Rev.*, **132**, 897–914, doi: [10.1175/1520-0493\(2004\)132<0897:ATV-DAS>2.0.CO;2](https://doi.org/10.1175/1520-0493(2004)132<0897:ATV-DAS>2.0.CO;2).
- Bauer, P., R. Buizza, C. Cardinali, et al., 2011: Impact of singular-vector-based satellite data thinning on NWP. *Quart. J. Roy. Meteor. Soc.*, **137**, 286–302, doi: [10.1002/qj.v137.655](https://doi.org/10.1002/qj.v137.655).
- Gratton, S., M. Rincon-Camacho, E. Simon, et al., 2015: Observation thinning in data assimilation computations. *EURO Journal on Computational Optimization*, **3**, 31–51, doi: [10.1007/s13675-014-0025-4](https://doi.org/10.1007/s13675-014-0025-4).
- Hilburn, K. A., F. J. Wentz, D. K. Smith, et al., 2006: Correcting active scatterometer data for the effects of rain using passive radiometer data. *J. Climate Appl. Meteor.*, **45**, 382–398, doi: [10.1175/JAM2357.1](https://doi.org/10.1175/JAM2357.1).
- Li, X. C., J. Zhu, Y. G. Xiao, et al., 2010: A model-based observation-thinning scheme for the assimilation of high-resolution SST in the shelf and coastal seas around China. *J. Atmos. Oceanic Technol.*, **27**, 1044–1058, doi: [10.1175/2010JTECHO709.1](https://doi.org/10.1175/2010JTECHO709.1).
- Lin, M. S., X. W. Jiang, and X. T. Xie, 2010: Simulation of HY-2 scatterometer and analysis of wind field retrieval. Proceedings of the SPIE 7807, Earth Observing Systems XV, San Diego, California, United States, 23 September, SPIE, 78070X.
- Lin, M. S., J. H. Zou, X. T. Xie, et al., 2013: HY-2A microwave scatterometer wind retrieval algorithm. *Engineering Sciences*, **15**, 68–74. (in Chinese)
- Ochotta, T., C. Gebhardt, D. Saupe, et al., 2005: Adaptive thinning of atmospheric observations in data assimilation with vector quantization and filtering methods. *Quart. J. Roy. Meteor. Soc.*, **131**, 3427–3437, doi: [10.1256/qj.05.94](https://doi.org/10.1256/qj.05.94).
- Prasad, V. S., A. Gupta, E. N. Rajagopal, et al., 2013: Impact of OSCAT surface wind data on T574L64 assimilation and forecasting system—A study involving tropical cyclone Thane. *Curr. Sci.*, **104**, 627–631.

- Rogers, R., S. Y. Chen, J. Tenerelli, et al., 2003: A numerical study of the impact of vertical shear on the distribution of rainfall in Hurricane Bonnie (1998). *Mon. Wea. Rev.*, **131**, 1577–1599, doi: [10.1175/2546.1](https://doi.org/10.1175/2546.1).
- Vogelzang, J., 2007: Two dimensional variational ambiguity removal (2DVAR). Technical Report NWPSAF-KN-TR-004, EUMETSAT, 62 pp.
- Wang, X. N., L. X. Liu, H. Q. Shi, et al., 2012: In-orbit calibration and performance evaluation of HY-2 scatterometer. Proceedings of IEEE International on Geoscience and Remote Sensing Symposium (IGARSS), Munich, 22–27 July, IEEE, 4614–4616.
- Yu, Y., W. M. Zhang, Z. Y. Wu, et al., 2015: Assimilation of HY-2A scatterometer sea surface wind data in a 3DVAR data assimilation system—A case study of Typhoon Bolaven. *Front. Earth Sci.*, **9**, 192–201, doi: [10.1007/s11707-014-0461-8](https://doi.org/10.1007/s11707-014-0461-8).
- Zhang, F. Q., Y. H. Weng, J. A. Sippel, et al., 2009: Cloud-resolving hurricane initialization and prediction through assimilation of Doppler radar observations with an ensemble Kalman filter. *Mon. Wea. Rev.*, **137**, 2105–2125, doi: [10.1175/2009MWR2645.1](https://doi.org/10.1175/2009MWR2645.1).
- Zhang, L., S. X. Huang, Y. D. Liu, et al., 2010: Variational assimilation combined with generalized variational optimization analysis for sea surface wind retrieval from microwave scatterometer data. *Acta Phys. Sinica*, **59**, 2889–2897. (in Chinese)
- Zhang, Y., M. S. Lin, Q. T. Song, et al., 2013: Research on the preprocessing of HY-2A space-borne scatterometer data. *Engineering Sciences*, **15**, 62–67. (in Chinese)

Tech & Copy Editor: Shuri LI
Language Editor: Colin SMITH